

ANALYSIS OF THE ROCK LAYER CONTACT USING THE GRAVITY DATA OF SATELLITE IMAGERY AND RESISTIVITY METHOD

Muwardi Sutasoma^{1*}, Adi Susilo¹, Sunaryo¹, Eko Andi Suryo², Suhayat Minardi³

¹Faculty of Science, Brawijaya University, Malang, Indonesia

²Faculty of Engineering, Brawijaya University, Malang, Indonesia.

³Faculty of Science, University of Mataram, Mataram, Indonesia

*Corresponding Author, Received: 15 Feb. 2022, Revised: 22 May 2022, Accepted: 12 June 2022

ABSTRACT. Research with the gravity data of satellite imagery and resistivity methods, Schlumberger configuration in the area of Sutami dam, and its surroundings has been undertaken. This study aims to determine the types of rock layer contact between limestone sediments and volcanic sediments for disaster mitigation. The Gravity data of satellite imagery was obtained from the Global Gravity Model Plus (GGMplus). The research area was 15 km x 15 km; the space between the points was 300 meters with 3000 measurement points. Resistivity data was obtained with an MAE type A6000E resistivity meter; the number of research points was 2 sounding points arranged in parallel to get 2D data. The location of data collection with the resistivity method, Schlumberger configuration was determined based on the results of research using gravity data of satellite imagery. Complete Bouguer anomaly values ranged from 73.6 mGal-89.3 mGal. The northern part of the research location has a lower Complete Bouguer anomaly than the southern area. It was because the northern part of the study area was part of volcanic sediment, although it was only on the surface, and the southern part was part of limestone sediment. Based on the value of resistivity data, the types of rock at research points 01 and 02 were soil, limestone, and sandy limestone. It was because the research point was located in a Campurdarat Formation. The results indicate that the contact layer between limestone and volcanic sedimentaries is located in: Campurdarat Formation, Wuni Formation, and the Butak Volcanic Product; Nampol Formation and Tuff Deposit; Tuff Deposit and Campurdarat Formation. This contact layer is more difficult to consolidate, so infrastructures built on it are more vulnerable.

Keywords: Sutami Dam, Rock Layer Contact, Gravity of Satellite Imagery, Resistivity

1. INTRODUCTION

Malang Regency is an area prone to natural disasters, especially earthquakes and ground movements. Due to the large number of earth faults that pass through it, this area is unstable [1] and prone to ground movement [2].

One area prone to ground movement is the Sutami Dam area and its surroundings. This dam is located in Karangates Village, Sumberpucung District, Malang Regency. This dam was built from 1964 to 1973 and started operating in 1977 [2]. The length of the embankment of this dam is 823.5 meters; the width is 13.7 meters, and it is located at an altitude of 188-387 meters (Above Sea Level) [2].

The Sutami Dam is an essential infrastructure in East Java Province, Indonesia. Together with the Lahor Dam, located to the north of the Sutami Dam, both are used as hydropower plants. They can contribute around 400 kWh of power per year from the total demand of around 52,263 MW installed throughout Indonesia in the last five years until 2020 [3].

Apart from being a hydropower plant, the Sutami dam is also used for tourist spots, irrigation, and

flood control. Because it is a vital infrastructure, the safety of the Sutami Dam needs to be considered energy sustainable. Dam safety is related to the subsurface geological structure and hydrostatic pressure.

Hydrostatic pressure affects the contact of the subsurface soil layer, and its magnitude depends on the depth of a compressive area at a certain depth [4]. The dam is an infrastructure that has a large hydrostatic pressure because there is water on its surface. Thus, it is necessary to research the types of rock layers below the surface [4].

Dams located in homogeneous areas have more resistance to hydrostatic pressure than dams located in non-homogeneous areas. In a dam located in a non-homogeneous area, the contact layer filled with water will reduce cohesion and increase lateral pressure due to hydrostatic pressure [4]. The Sutami Dam is located in a non-homogeneous area, namely the contact layer between Volcanic Sediment and Limestone sediment [5]. In addition, there is a weak zone in the western part of the Sutami Dam area. This weak zone is indicated by the presence of the Selorejo-Kalirejo fault and the shallow effect of the Selorejo-Kalirejo fault and the Pohgajih-Kalirejo

North shear fault [6]. Every year, in the Pohgajih area, which is located close to the Sutami Dam, occurs fault activity causes houses to crack. [7]. Sutami Dam is also classified as a dam with a high level of risk. The problem that often occurs in this dam is the existence of elongated cracks at the dam's top. This crack appeared during construction and lasted until it was finished, around 1969-1971. This crack reoccurred in 2014. It is known from the results of visual observations in 2014 that there was an elongated crack at the dam's top along 120 m and had a depth of 1.5 meters - 2 meters from the surface [8]. The results of the study using the resistivity method upstream and downstream of the dam revealed a distribution of fracture zones scattered on the dam's surface to a depth of 8-18 meters, both upstream and downstream. It is indicated by a low resistivity value ranging from 0,922 Ω m to 9,57 Ω m. The results of 3D data processing also revealed that the crack zone had spread between the upstream and downstream sections, namely the roadway at the top of Sutami Dam [1]. It caused the Sutami dam to become unstable [9]. Thus, further research is needed using geophysical methods to determine the types of rock layers below the surface and the geological structure in the area around the Sutami dam for disaster mitigation.

The geophysical methods used in this study were the gravity method of satellite imagery and the resistivity method, the Schlumberger configuration. The gravity method was used to measure rocks' density properties below the surface, which were influenced by its gravity field, while the resistivity method was used to estimate subsurface geological conditions by utilizing the nature of electric currents in rocks with the earth being used as a conductor [10]. Density and resistivity have values that vary from one material to another. Because of this variation, measuring the density and resistivity of unknown material is potentially very useful in identifying the material, with little more information [11-12]. In addition, the geomagnetic method can determine the depth and structure of the subsurface so that a clearer local and regional anomaly can be obtained [13].

Therefore, it is necessary to conduct research using gravity data of satellite imagery and resistivity methods to determine the rock layer contact between limestone and volcanic sediments. The aim of this research is to show how the response of infrastructures built between limestone and volcanic sediments. The results, in turn, can be used as recommendations for the government to determine policies regarding disasters.

2. RESEARCH SIGNIFICANCE

Dams are essential infrastructure because they can be used for power plants, irrigation, tourist attractions, and flood control.

Dam construction should pay attention to subsurface rock structures. It has to do with the dam's safety. Dams built in homogeneous areas have a stronger resistance to hydrostatic pressure than dams located in non-homogeneous areas.

This research can be an input for the government to determine the location of dam construction by paying attention to the rock structure below the surface. For dams built in non-homogeneous areas, this research can be input so that the government pays more attention to and periodically evaluates the community's safety around the dam.

3. FIELD SITE STUDY

The geological map in Fig. 1 shows that the location of the study consisted of Tuff Deposit (Qptm), Butak Volcanic Products (Qpkb,) Nampol Formation (Tmn), Wuni Formation (Tmw), and Campurdarat Formation (Tmcl). Qptm consisted of tuff lapilli, pumice tuff, and lava. Qpkb consisted of lava, volcanic breccia, tuff breccia, and tuff sandstone. Tmn consisted of sandstone, tuff, clay, and marl. Tmw consisted of andesite-basalt breccias, breccia lava andesite lava and tuff sandstone inserts. Tmcl consisted of crystalline limestone and claystone insertion. The location of the dam was also closed to the Pohgajih Local Shear Fault, the Selorejo Local Fault, and the Selorejo limestone-andesite contact area [14].

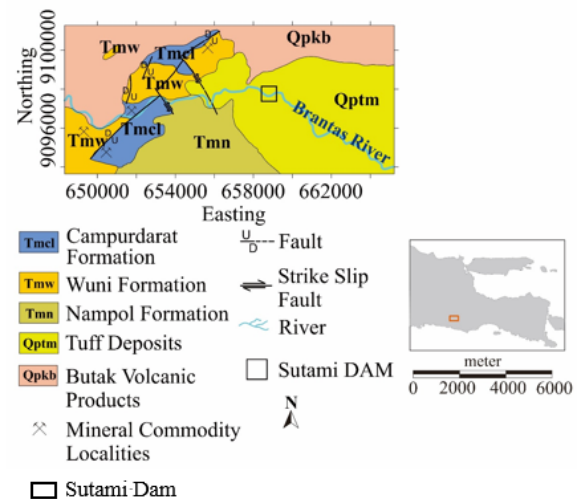


Fig. 1 Geological Map of Research Area [6]

4. METHOD

The research was conducted in October 2021 using the gravity data of satellite imagery and resistivity method, Schlumberger configuration to obtain sounding data. The research area using the gravity data of satellite imagery was 15 x 15 Km; the space between research points was 220 m, and the data was 3000 measurement points. The Gravity data of satellite imagery was downloaded from Global

Gravity Model Plus (GGMplus). GGMPlus is a gravitational field model taken from the GOCE satellite (TIM-4), GRACE satellite data (ITG2010), EGM2008, and gravity topography [15]. The data was obtained in the form of latitude and longitude positions, altitude, and Free Air Anomaly (FAA). Research using the resistivity method, Schlumberger configuration was carried out in Kalirejo Village, Kalipare District, Malang Regency, with 2 sounding points arranged parallel to obtain 2D data.

4.1 Gravity Method

The gravity data of Satellite imagery was obtained from GGMPlus satellite data (Global Gravity Model Plus). The research area was 15 km x 15 km with a space between points of 220 m. The amount of data was 3000 measurement points.

The main principle in gravity method research is Newton's law of attraction. Where the magnitude of the gravitational force between two masses m_1 and m_2 is separated by a distance of r can be written as [16],

$$\vec{F} = -\gamma \frac{m_1 m_2}{r^2} \hat{r} \quad (1)$$

Where \vec{F} is the force (N); m_1 and m_2 are the mass of the object (kg); r is the distance between two objects; \hat{r} is the unit vector from m_1 to m_2 , and γ is the universal gravitational constant ($6.67 \times 10^{-11} \text{ m}^3 \text{ kg}^{-1} \text{ s}^{-2}$).

The result of the measurement using the gravity method is a complete Bouguer anomaly. The complete Bouguer anomaly (CBA) is the difference between the observed gravitational value and the theoretical gravity value that should be observed at a point. Gravitational anomalies show variations in the acceleration of the earth's gravity caused by lateral variations in the density of the earth's layers. The Complete Bouguer Anomaly can be written as [16],

$$CBA = g_{sta} - (g\phi + FAC + BC - TC) \quad (2)$$

$$= g_{sta} - g\phi + (0.3086 - 0.04193\rho)h + TC \quad (3)$$

Where g_{sta} is the value of gravity at the point of observation; $g\phi$ is the value of theoretical gravity; FAC is Free Air Correction; BC is Bouguer Correction; TC is Terrain Correction; ρ is the average rock mass density; h is the height of the observation point above sea level.

The Complete Bouguer Anomaly is still present at various altitudes in the research area. The effect of this variation in altitude position distorts the value of the gravitational field.

A complete Bouguer anomaly reduction process is accomplished to a flat plane to minimize distortion and facilitate data interpretation. Reduction to a flat plane is the process of bringing a Bouguer anomalous value that is still affected topographically to a flat plane at a particular altitude [17].

The upward continuation process is carried out after reducing the flat plane on the complete Bouguer anomaly. Upward continuation is the step of converting potential field data measured at a surface level into data that seems to be measured at a higher surface level [18]. Upward continuum is also one of the methods used as a filter to remove noise generated by objects near the surface. Flat field reduction produces regional anomalies and residual anomalies. Regional anomalies are heavy force anomalies caused by differences in rock density in deep regions. Residual anomalies are heavy force anomalies caused by differences in rock density in shallow areas.

Data processing begins by creating Bouguer anomalous map using Oasis Montaj software. Then, modeling is done to obtain a 2D profile using Grav3D software.

4.2 Resistivity Method

Research using the resistivity method, Schlumberger configuration was carried out in Kalirejo Village, Kalipare District, Malang Regency in October 2021. The tool used was the MAE type A6000E resistivity meter.

The resistivity method is a method that makes use of the earth's electrical properties with the resistivity of subsurface rocks as parameters. This method is an active method in which the current is injected into the earth via two current electrodes (C1 and C2), and the resulting potential is caught by two potential electrodes (P1 and P2). Considering the geometry factors used, the pseudo-resistivity value beneath the surface can be calculated. The results of the data processing of this method will show the subsurface lithology, which can show the types of rocks that make up the subsurface of the research area [19].

This research applied the Schlumberger configuration. This configuration can obtain data using Vertical Electrical Sounding (VES), so the resistivity data obtained is deeper and matches the research target. The ability to detect the non-homogeneity of rock layers on the surface is the advantage of the Schlumberger configuration [20].

The Schlumberger configuration is a configuration that has an electrode current greater than the potential electrode distance. The arrangement of the Schlumberger array can be seen in Fig. 2.

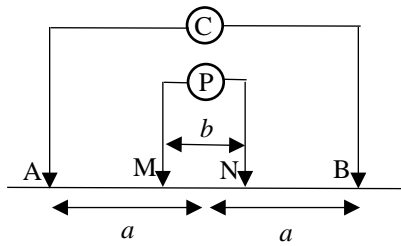


Fig 2. Schlumberger Array

In Figure 2, A represents the positive current electrode, B represents the negative current electrode, M represents the positive potential electrode, and N represents the negative potential electrode. The apparent resistivity value in the geoelectric resistivity measurement method with the Schlumberger configuration can be written as [9],

$$\rho_{\alpha} = k \frac{V}{I} \quad (4)$$

ρ_{α} is the apparent resistivity value, k is the geometry factor, V is the potential difference (millivolts), I is the current injected (milliampere).

The value of k in the Schlumberger configuration can be written as,

$$k = 2\pi \left\{ \left(\frac{1}{r_1} - \frac{1}{r_2} \right) - \left(\frac{1}{r_3} - \frac{1}{r_4} \right) \right\}^{-1} \quad (5)$$

r_n ($n = 1,2,3,4$) is an inter-electrode spacing owned; r_1 is distance A with M, r_2 M with B, r_3 N with A, and r_4 N with B. Thus, the geometry factor of the Schlumberger array can be calculated by Eq. (6).

$$k = \pi \frac{a^2}{b^2} \left(1 - \frac{b^2}{4a^2} \right) \quad (6)$$

a is half the distance between A and B, and b is the distance between M and N. Data processing of Schlumberger's configuration resistivity used IP2Win and Progress3 software.

5. RESULTS AND DISCUSSION

5.1 Result

5.1.1 Gravity Data of Satellite Imagery

Data interpretation of the anomaly gravity data used a qualitative and quantitative approach. The qualitative interpretation was carried out by reading the contours of the gravity anomaly originating from objects below the earth's surface. In contrast, quantitative interpretation was made by creating a 2D profile of the residual anomalies.

a. Complete Bouguer Anomaly (CBA)

Complete Bouguer Anomaly (Fig. 3) is an anomaly caused by subsurface rock density. CBA

values obtained after various corrections represent the combined response of various masses located in the area around the Sutami Dam. CBA has a minimum value of 73.6 mGal and a maximum value of 88.7 mGal.

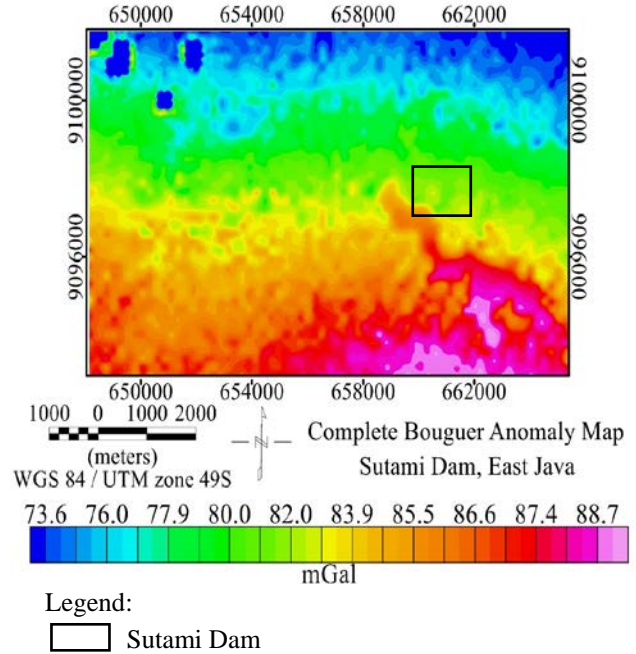


Fig. 3 Complete Bouguer Anomaly

Based on the range of Anomaly values in complete Bouguer anomaly, anomalies can be divided into two groups, namely low anomalies and high anomalies. The low anomaly in the north has a value between 73.6 mGal - 82.0 mGal. This anomaly is estimated to be a combination of several formations, such as the Campurdarat Formation, Nampol formation, and Wuni formation. The Campurdarat Formation (Tmcl) is above the tuff member of the Mandalika Formation. The Campurdarat Formation consists of crystalline limestone and claystone inserts. The Nampol Formation (Tmn) consists of tuffaceous-limestone sandstone, claystone, and marl. The Wuni Formation (Tmw) is dominated by ancient volcanic eruption rocks and deposited above the Campurdarat Formation. This formation consists of andesite-basalt breccia, breccia lava, andesite lava, and tuffaceous sandstone inserts.

The high anomaly in the south has a value between 82.0 mGal-88.7 mGal. This anomaly is estimated to consist of the Campurdarat Formation and the tuff members of the Mandalika Formation, both of which are in the late Oligocene to early Miocene age. The Mandalika Formation consists of andesite-basalt lava, porphyry latit, rhyolite, and dacite. The tuff members of the Mandalika Formation consist of glass tuff, crystal tuff, and breccia tuff, which are generally pumice rock.

b. Regional Gravity Anomaly

Regional gravity anomaly is caused by deep anomalies that have low frequencies and long wavelengths [16]. Based on Fig. 4, the regional anomaly has a minimum value of 72.3 mGal and a maximum value of 88.6 mGal.

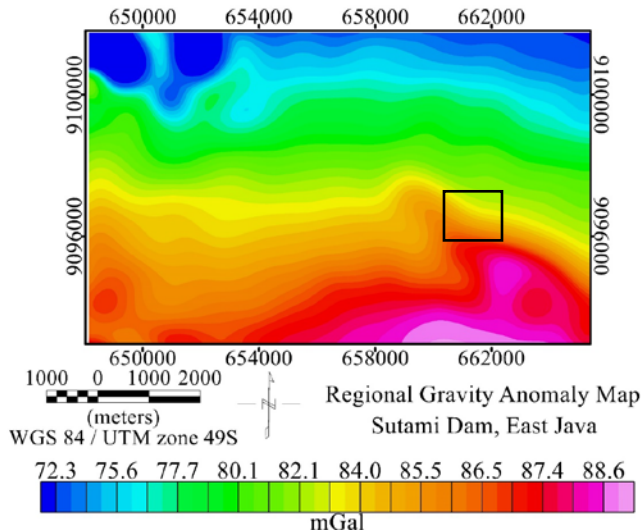


Fig. 4 Regional Gravity Anomaly

The anomaly value in the north is lower than in the south. The low anomaly to the north between 72.3 mGal - 82.1 mGal is thought to be limestone sedimentary rock. The high anomaly in the southern part between 84.1 mGal - 88.6 mGal are thought to be volcanic sedimentary rocks. In the southern part of the research area, there are many ancient volcanoes such as Mount Pehlembun, Mount Soko, Mount Kiki, Mount Korowedhus, and Mount Tretes.

c. Residual Gravity Anomaly

Residual gravity anomaly is caused by shallow anomalies with high frequencies and short wavelengths [16]. Residual anomaly maps are analyzed by correlating with Blitar regional geological maps.

Based on Fig. 5, The residual anomaly has a minimum value of -1.7 mGal to 1.8 mGal. The high anomaly in the northwest area is caused by ancient volcanoes, namely Mount Selorejo, Mount Sedayu, and Mount Golo. In contrast, high anomalies in the southern regions are part of the Mandalika Formation.

d. 2D Profile in Study Area

The quantitative interpretation was carried out by slicing on the residual anomaly of the gravity data of satellite imagery and comparing it with the result of slicing in previous studies with the magnetic method [5].

It causes the Wuni Formation to be cut off by an overland formation and reappear on the surface. In

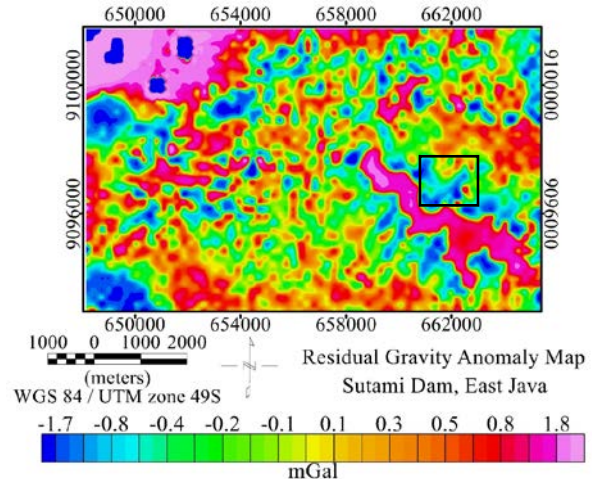


Fig.5 Residual Gravity Anomaly

There are three slices in this study, namely: slicing a-a', slicing b-b,' and slicing c-c.' The location of the slicing can be seen in Fig. 6. The slicing location is selected from the high anomaly to the low anomaly and represents the northern and southern parts of the research area. In addition, slicing is carried out through the Sutami Dam.

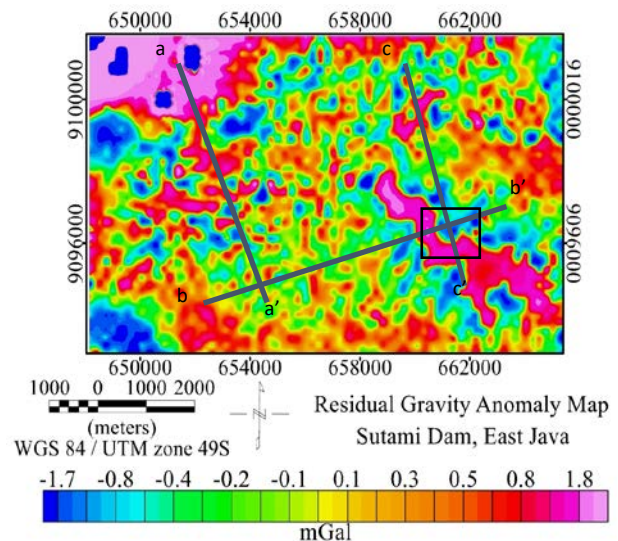


Fig.6 Slice on Residual Gravity Map

The rock formations in the 2D profile a-a' (Fig. 7) consist of Butak Volcanic Product, Wuni Formation, Campurdarat Formation, Nampol Formation, and Mandalika Formation. The type of formation in this area is in line with the results of previous studies using magnetic data [5].

This area is an area of ancient volcanoes such as Mount Pahlembun and Mount Soko.

in addition, some faults cut Butak Volcanic Products, Wuni Formation, and Campurdarat Formation.

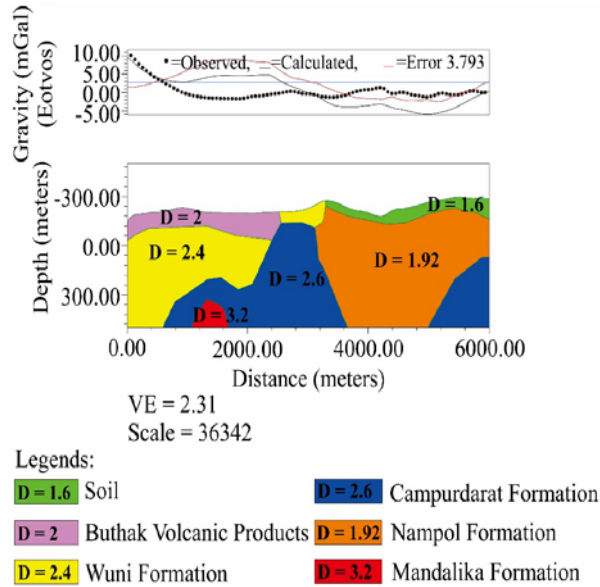


Fig. 7 2D profile a-a'

The rock formations in the 2D profile b-b' (Fig. 8) are Campurdarat Formation, Nampol Formation, and Tuff Deposit. The type of formation in this area follows the results of previous studies using magnetic data [5]. The Sutami Dam was built on top of the Tuff Deposit adjacent to the Nampol Formation to its west.

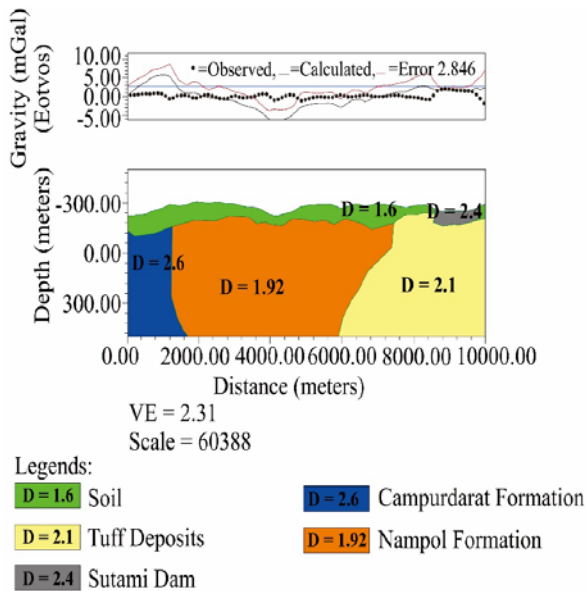


Fig. 8 2D profile b-b'

The rock formations in 2D Profile c-c' (Fig. 9) are Butak Volcanic Product, Tuff Deposit, and Campurdarat Formation. This type of formation in 2D Profile c-c' corresponds to the results of previous research slicing using magnetic data [5] and the results of pseudo gravity data slicing [21].

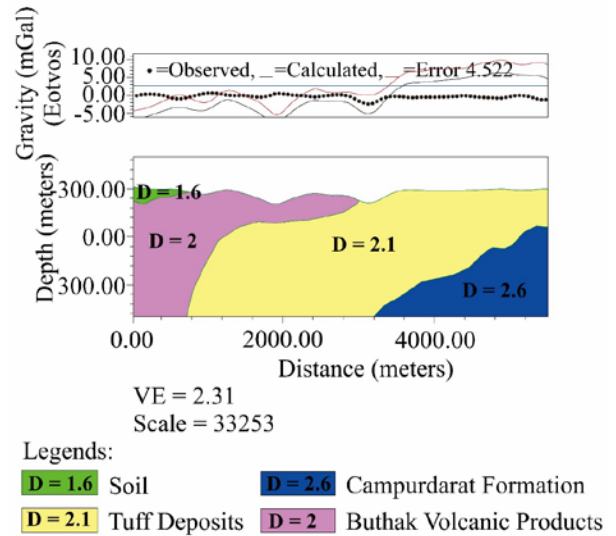


Fig. 9 2D profile c-c'

5.1.2 Resistivity Method

Data interpretation of the resistivity data used a quantitative approach. The quantitative interpretation was carried out by making a 1D model from the data of two research points and arranged in parallel to obtain 2D data.

Based on 2D profile b-b' in the gravity data of satellite imagery, the location of the resistivity method data collection was carried out in the area of Campurdarat formations (Fig. 10).

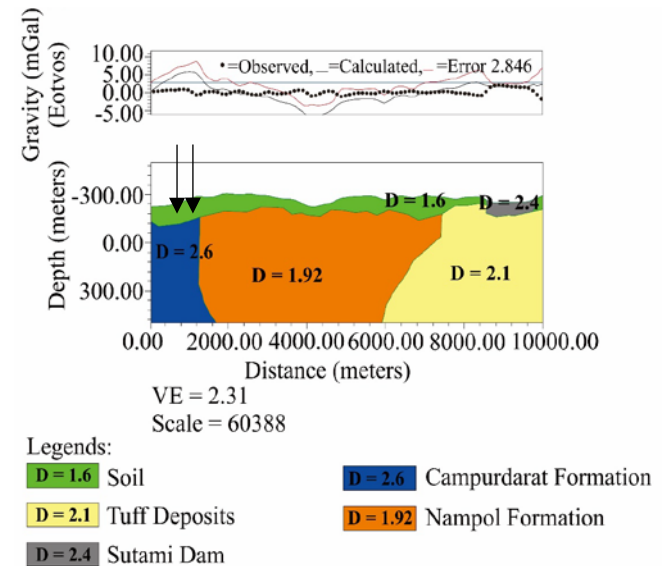


Fig. 10 Location of Data Collection Resistivity Method (Mark in arrow)

The data collection points are two sounding points arranged parallel to obtain a 2D cross-section. Jarak antar kedua titik sounding adalah sekitar 200 m.

The types of rock layers using the resistivity method can be seen in table 1 and table 2.

Table 1. Interpretation of results at VES point 1

Layer	Depth (m)	Resistivity (Ωm)	Type of rock
1	0-2	19.9	Soil
2	2-109	131	Limestone
3	109-160	45.9	Sandy Limestone

Table 2. Interpretation of results at VES point 2

Layer	Depth (m)	Resistivity (Ωm)	Type of rock
1	0-4	24	Soil
2	4-203	1224	Limestone
3	203-290	546	Sandy Limestone

The types of rocks at VES Point 1 and VES Point 2 are soil, limestone, and sandy limestone. These three rocks belong to the type of limestone sediments and are in line with the 2D cross-section of the results of slicing gravity data from satellite imagery. It shows that the results of slicing gravity data of satellite imagery are confirmed by the resistivity method.

Based on the 2D Cross Section on the resistivity method data, there are three rock layers, namely soil (first layer), limestone (second layer), and sandy limestone (third layer). The types of rock layers in this area are in line with the types of rock in the Campurdarat Formation.

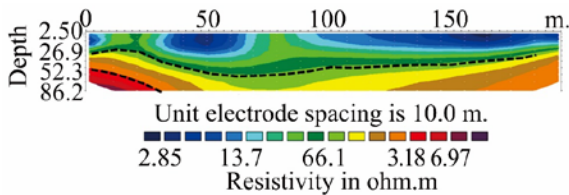


Fig. 11 2D Cross Section in Kalirejo Village (Parallel between VES point 1 and VES Point 2)

5.2 Discussion

Based on 2D profile a-a' (Fig.7), the contact layer between limestone and volcanic sediments is between the Campurdarat Formation and the Wuni Formation, and the Butak Volcanic Product. Commonly, the Campurdarat Formation is under the Wuni Formation and Butak Volcanic Product, so it suffers a bigger load and is more consolidated than the formation above it [6]. It causes the contact layer between limestone and volcanic sediments to become less consolidated, so it is more vulnerable.

Based on 2D profile b-b' (Fig.8), the contact layer between limestone and volcanic sediment is located in the west of the Sutami Dam, which is between the Tuff Deposit and the Nampol Formation. Commonly, the Nampol Formation is located under the Tuff Deposit, so it gets a bigger load than the formation above it. It causes the contact layer between limestone sediment and volcanic sediment to become less cohesive, causing the western part of the Sutami Dam to be included in the weak zone [22]. In addition, 2d profile c-c'.

6. CONCLUSIONS

Infrastructure built on contact layers of limestone and volcanic sediment is more vulnerable than infrastructure built on homogeneous rock layers. This is because the limestone sediment layer is below the volcanic sediment layer, causing the limestone sediment to get a greater load than the rock layer above it. In addition, the contact layer between limestone sediments and volcanic sediments becomes less cohesive and causes the bonds between rock layers to become weaker.

So, The government needs to pay attention and evaluate periodically for security. For further researchers, it is necessary to carry out laboratory tests to determine the strength of the contact layer between limestone and volcanic sediments.

7. ACKNOWLEDGMENTS

The author would like to thank the Faculty of Mathematics and Natural Sciences, Brawijaya University, for funding this research through the Non-tax state revenue (PNBP) of Brawijaya University in line with the Budget Implementation List (DIPA) of Brawijaya University Number DIPA-023.17.2.677512/2021 and Professor and Doctoral Research Grant Contract for the Fiscal Year 2021 Number 1586/UN10.F09/PN/2021.

8. REFERENCES

[1] Fitriah F., Sunaryo, and Susilo A., Identification of Cracked Zone in Sutami dam Using Geoelectrical Method, Indonesian Journal of Applied Physics, Vol. 5, No. 02, 2015, pp. 65–72.
 [2] Purwana Y. M., Raden Harya D.H.I, Setiawan B., and Aulawi N., Seismic Hazard Analysis for Sutami Dam using Probabilistic Method. MATEC Web of Conferences, Vol. 12, 2019, pp. 1–9.
 [3] [https://web.pln.co.id/statics/uploads/2021/04/St statistik-Indonesia-2020-unaudited.pdf](https://web.pln.co.id/statics/uploads/2021/04/St%20statistik-Indonesia-2020-unaudited.pdf) 2021 access date 18 March 2021

- [4] Hardiyatmo, Hary C., *Mekanika Tanah 1*, Gadjah Mada University Press, 2012, pp.200-282.
- [5] Sutasoma M., Susilo A., Sunaryo, Sarjiyana, Cahyo R. H. D., Suryo E. A., Identification of Rock Layer Contacts in the Surrounding of the Sutami Dam Using Geomagnetic Methods, *International Journal of GEOMATE*, Vol. 21, No. 84, 2021 pp. 188–193.
- [6] Sjarifudin S. and Hamidi, *Peta Geologi Lembar Blitar, Jawa*. Pusat Penelitian dan Pengembangan Geologi, Bandung, 1992.
- [7] Susilo A., Sunaryo, Fitriah F., and Sarjiyana, Fault Analysis in Pohgajih Village , Blitar , Indonesia, *International Journal of GEOMATE*, Vol. 14, No. 41, 2018, pp. 111–118.
- [8] Indrawan D., Tanjung M.I., Setyawan H.E., Sadikin N., Static and Dynamic Analysis of Longitudinal Crack on Crest, *Jurnal Teknik Hidraulik*, Vol. 6, No. 1, 2015, pp. 77–90,
- [9] Sunaryo and Susilo A., Seepage Zone Identification at Sutami Dam using Geoelectrical Resistivity Data, *IOP Conference Series: Earth and Environmental Science*, Vol. 012011, No. 75, 2017, pp. 1–6.
- [10] Rahmani T. R., Sari D. P., Akmam A., Amir H., and Putra A., Using the Schlumberger configuration resistivity geoelectric method to analyze the characteristics of slip surface at Solok, *Journal of Physics Conference Series*, Vol. 1481(012030), 2020, pp. 1-9.
- [11] Rohadi S., Sakya A.E., Masturyono, Murjaya J., Sunardi B., Rasmid, Ngadmanto D., Susilanto P., Nugraha J., Pakpahan S., Ground landslide hazard potency using geoelectrical resistivity analysis and VS30, a case study at the geophysical station, Lembang, Bandung, AIP Conference Proceeding., Vol. 1857, No. 060004-1–060004-7, 2017, pp. 1–8.
- [12] Yanis M., Marwan, The potential use of satellite gravity data for oil prospecting in Tanimbar Basin, Eastern Indonesia, *IOP Conference Series: Earth and Environment Science*. Vol. 364, No. 1, 2019, pp. 1-7.
- [13] Burger H. R., Sheehan A. F., and Jones C., *Introduction to Applied Geophysics: Exploring the Shallow Subsurface*, Prentice Hall PTR, 1992, pp. 389–452.
- [14] Sunaryo and Susilo A., Vulnerability of Karangates Dams Area using Zero Crossing Analysis of Data Magnetic, *AIP Conference Proceedings*, Vol. 1658, No. 060007, 2015, pp. 1–8.
- [15] Suprianto, A., Supriyadi, Priyantari, N., & Cahyono, B. E, Correlation between GGMPPlus, topic and BGI gravity data in volcanic areas of Java Island, *Journal of Physics: Conference Series*, Vol. 1825(012023), 2021, pp. 1–6.
- [16] Telford W. M., Geldart R. E., and Sheriff L.P., *Applied Geophysics*, Second Edition, Cambridge University Press, 1990, pp. 6-61
- [17] Setyawan A., *Kajian Metode Sumber Ekuivalen Titik Massa Pada Proses Pengangkatan Data Gravitasi Ke Bidang Datar*, *Berkala Fisika*, vol. 8, No. 1, 2005 pp. 7–10.
- [18] Blakely R. J., *Potential Theory in Gravity and Magnetic*, Cambridge University Press, 1995, pp. 313–356.
- [19] Susilo A., Fitriah F, Sunaryo, Rachmawati E. T. A, and Suryo E. A., Analysis of landslide area of Tulung subdistrict, Ponorogo, Indonesia in 2017 using resistivity method, *Smart Sustainable Built Environment*, Vol. 9, No. 4, 2020 pp. 341–360.
- [20] Sutasoma M., Azhari A. P., dan Arisalwadi M., Identifikasi Air Tanah Dengan Metode Geolistrik Resistivitas Konfigurasi Schlumberger Di Candi Dasa Provinsi Bali, *Konstan - Jurnal Fisika Dan Pendidik. Fisika*, Vol. 3, No. 2, 2018 pp. 58–65.
- [21] Sunaryo and Susilo A., Vulnerability of Karangates Dams Area using Density Contrast Parameter to Anticipate Energy Sustainability, in *Basic Science*, Vol. 5. Issue 9, 2015, pp. 1689–1699..
- [22] Sutasoma M., Susilo A., Sunaryo, Suryo E. A., Minardi S., and Cahyo R. H. D., Comparison between the magnetic method data of pseudo gravity transformation with gravity anomaly data from satellite imagery in the surrounding of the Sutami Dam to identify subsurface formations, in *Journal of Physics Conference Series*, Vol. 2165, No. 01201, 2022, pp. 1–9.